ISSN 1674-1056
http://cpb.iphy.ac.cn
http://iopscience.iop.org/cpb
中国物理 B
Chinese Physics
中国物理
Chinese Physics B

Beryllium carbide as diffusion barrier against Cu: First-principles study

Hua-Liang Cao(曹华亮)[1], Xin-Lu Cheng(程新路)[1,2], Hong Zhang(张红)[1,2]

Citation: Chin. Phys. B . 2020, 29(1): 016601 . **doi:** 10.1088/1674-1056/ab593e
Journal homepage: http://cpb.iphy.ac.cn; http://iopscience.iop.org/cpb

What follows is a list of articles you may be interested in

Benchmarking PBE+D3 and SCAN+rVV10 methods using potential energy surfaces generated with MP2+ΔCCSD(T) calculation

Jie Chen(陈劼)[1,2], Weiyu Xie(谢炜宇)[3], Kaihang Li(李开航)[1], Shengbai Zhang(张绳百)[4], Yi-Yang Sun(孙宜阳)[2]
Chin. Phys. B . 2020, 29(1): 013102 . **doi:** 10.1088/1674-1056/ab5fbb

An analytical model of thermal mechanical stress induced by through silicon via

Dong Gang, Shi Tao, Zhao Ying-Bo, Yang Yin-Tang
Chin. Phys. B . 2015, 24(5): 056601 . **doi:** 10.1088/1674-1056/24/5/056601

Quantum diffusion in bilateral doped chains

Jin Fu-Bao, Zhang Kai-Wang, Zhong Jian-Xin
Chin. Phys. B . 2011, 20(7): 076701 . **doi:** 10.1088/1674-1056/20/7/076701

Beryllium carbide as diffusion barrier against Cu: First-principles study*

Hua-Liang Cao(曹华亮)[1], Xin-Lu Cheng(程新路)[1,2], and Hong Zhang(张红)[1,2,†]

[1] *Institute of Atomic and Molecular Physics, Sichuan University, Chengdu* 610065, *China*
[2] *College of Physics, Sichuan University, Chengdu* 610065, *China*

(Received 22 October 2019; revised manuscript received 18 November 2019; accepted manuscript online 20 November 2019)

Beryllium carbide is used in inertial confinement fusion (ICF) capsule ablation material due to its low atomic number, low opacity, and high melting point properties. We used the method of climbing image nudged elastic band (CINEB) to calculate the diffusion barrier of copper atom in the crystal of beryllium and beryllium carbide. The diffusion barrier of copper atom in crystal beryllium is only 0.79 eV, and the barrier in beryllium carbide is larger than 2.85 eV. The three structures of beryllium carbide: anti-fluorite Be_2C, Be_2C-I, and Be_2C-III have a good blocking effect to the diffusion of copper atom. Among them, the Be_2C-III structure has the highest diffusion barrier of 6.09 eV. Our research can provide useful help for studying Cu diffusion barrier materials.

Keywords: diffusion barrier, beryllium carbide, adsorption energy

PACS: 66.30.Ny, 67.80.dj, 31.15.eg **DOI:** 10.1088/1674-1056/ab593e

1. Introduction

Beryllium is the first wall in the fusion reactor[1,2] and was considered as a candidate material for ICF, which has the advantages of high density, low opacity, high melting point, and high thermal conductivity,[3,4] and it has a high ablation rate due to these advantages. It is more beneficial for implosion coupling efficiency and can suppress the growth of ablation instability in indirect-drive inertial confinement fusion.[5–8] In order to optimize the shock timing of the capsule, a five-layer gradient Cu-doped structure was designed.[9] The copper has better penetrability to x-rays, prevents x-rays from preheating the fuel, and helps control the shock timing.[9] The copper atoms exhibit uneven diffusion in the capsule during pyrolysis. This uneven distribution of copper can lead to Rayleigh–Taylor instability during the implosion process, which greatly reduces the performance of the capsule.[9,10] Low atomic number materials carbon, SiC, Be_2C, B_4C, TiC, BN, Si_3N_4, AL_2O_3, and BeO were considered for use as fusion materials.[11] In order to block the diffusion of copper inside the capsule, Hu *et al.* used *in situ* and *ex situ* oxide layer to prevent the diffusion of copper.[9] Liu *et al.* also analyzed the blocking effect of BeO on the diffusion of copper atoms by theoretical calculations.[12] However, it was observed that the interface in the capsule was layered and a large gap was created along the inner surface in the experiment, which seriously affected the shock timing.[9,10] Therefore, looking for new barrier materials is important. The formation of beryllium carbide films has been reported.[13–15] Recently, Luo *et al.*[16] prepared a Be_2C films by using a DC (reactive magnetron sputtering) method. The Be_2C films was also found to have high quality density, optical transmittance, and low surface roughness. Be_2C has low atomic number, better x-ray transmittance, higher mass density, and better thermal conductivity.[17] It has been found that Be_2C is highly resistant to radiation damage.[18] These properties meet the main requirements of the capsule in the ICF.[7,19] Beryllium carbide has three stable structures. The anti-fluorite Be_2C has been prepared and characterized.[20] The Be_2C-I and Be_2C-III structures were predicted by Li and Mosayeb *et al.*[21,22] using the method of first principles, respectively. However, the study of beryllium carbide in blocking the diffusion of Cu has not been reported.

In this paper, we calculate the diffusion activation energy of copper atoms in the crystal of beryllium using the method of first-principles study. Using the same method, we studied the diffusion barrier of copper atoms in three structures of beryllium carbide. It was found that the anti-fluorite Be_2C, Be_2C-I, and Be_2C-III can effectively block the diffusion of copper atoms, and the blocking effect of Be_2C-III is the best.

2. Computational methods

Our study based on the density functional theory (DFT) and the method of CINEB.[23,24] The program used is the Vienna *ab-initio* simulation package (VASP).[25,26] The exchange–correlation terms are described by Perdew–Burke–Ernzerhof (PBE) parameterization of the generalized gradient approximation (GGA).[27] The projector-augmented wave

*Project supported by the National Natural Science Foundation of China (Grant Nos. 11974253 and 11774248) and the National Key Technology Research and Development Program of the Ministry of Science and Technology of China (Grant No. 2017YFA0303600).

†Corresponding author. E-mail: hongzhang@scu.edu.cn

© 2020 Chinese Physical Society and IOP Publishing Ltd

potential[25] is employed to describe the electron–ion interactions. The accuracy of energy and force are 10^{-5} eV/atom and 0.02 eV/atom. It was tested that all structural models are converged when the plane-wave cutoff energy and the Gaussian broadening are set to 750 eV and 0.1 eV, respectively. The force of each image converges to less than 0.02 eV in the CINEB calculation. The integration in the Brillouin zone is automatically generated by the Monkhorst–Pack scheme,[28] and the k-point meshes of all structures were tested. The vdW correlation needs to be considered when obtaining the adsorption energy of copper atoms on the surface. We used the DFT-D2 method[29] in calculating the adsorption energy of copper atoms on the surface of beryllium carbide. The difference in energy is only 0.02 eV when considering the spin polarization. Therefore, the spin of electrons is not considered. According to geometric symmetry, there are two base plane and three non-base plane interstitial sites in the single crystal of beryllium.[30,31] As shown in Fig. 1, there are trigonal interstitial site (Tr) and hexahedral site (Hx) in the base plane, and octahedral site (Oc), tetrahedral site (Te), and non-basal trigonal interstitial site (NBt) in the non-base plane. As shown in Table 2 later, we calculated the formation energy of copper atoms in these five interstitial sites, and the copper atoms in the substitution site of the single crystal of beryllium. The formation energy of copper-doped single crystal of beryllium[32] reads

$$E_i^{\text{sub}} = E_{i,\text{Be}} - E_{\text{Be}}^{\text{Perf}} \times \frac{N-1}{N} - E_i^{\text{iso}}, \tag{1}$$

$$E_{\text{Cu}}^{\text{int}} = E_{\text{Cu,Be}} - E_{\text{Be}}^{\text{Perf}} - E_{\text{Cu}}^{\text{iso}}, \tag{2}$$

where E_i^{sub} is the formation energy of the point defect i in the substitutional site, and $E_{\text{Cu}}^{\text{int}}$ is the formation energy of an interstitial copper atom. i is a copper atom or a vacancy, $E_{i,\text{Be}}$ is the energy of the perfect of beryllium crystal containing a point defect i, $E_{\text{Be}}^{\text{Perf}}$ is the energy of a perfect supercell, and N is the number of atoms in a perfect supercell. $E_{\text{Cu}}^{\text{iso}}$ represents the energy of the isolated copper atom or zero when i represents a copper atom or a vacancy. $E_{\text{Cu,Be}}$ is the energy of the single crystal of beryllium containing an interstitial copper atom. We use the $4\times4\times3$ HCP supercell of beryllium and $5\times5\times5$ k-point mesh when calculating the diffusion activation energy of copper in the single crystal of beryllium. In the model of the interstitial mechanism, there are 96 beryllium atoms and 1 copper atom. The vacancy mechanism contains 94 beryllium atoms, one copper atom, and one beryllium vacancy. Three diffusion networks were chosen in the interstitial diffusion mechanism, where they are the copper atoms passing through the Oc site (Tr–Oc–Tr), the Hx site (Tr–Hx–Tr), and the NBt site (Tr–NBt–Tr) from the trigonal interstitial site (Tr), as shown in Figs. 2(a), 2(b), and 2(c). The copper in the initial structure was placed in the lowest energy position (Tr) in these three diffusion networks. Similarly, in the vacancy mechanism, we also chose three kinds of diffusion networks, in which the copper atom jumps to the nearest neighbor vacancy in basal plane (pathway-I), the nearest vacancy in non-basal plane (pathway-II), and the second adjacent vacancy (pathway-III), as shown in Figs. 2(d), 2(e), and 2(f). The thickness of the vacuum layer was set to 20 angstroms when the copper atoms were adsorbed on the beryllium carbide monolayers Be_2C-I and Be_2C-III, and the $4\times4\times1$ supercell of beryllium carbide was used. The adsorption energy E of Cu atoms on the surface of Be_2C-I and Be_2C-III can be expressed as follows:[33]

$$E_{\text{ad}} = E_{\text{Cu+sub}} - E_{\text{sub}} - E_{\text{Cu}}. \tag{3}$$

First, we calculated the diffusion activation energy of copper through the beryllium carbide monolayer (Be_2C-I and Be_2C-III) and the monolayers were placed in the crystal of beryllium. When the beryllium carbide monolayer was placed on the (0001) plane of the crystal of beryllium, the lattice mismatch is 0.22% (Be_2C-I) and 8.6% (Be_2C-III), respectively, and a k-point mesh of $5\times5\times5$ was utilized. In Fig. 7 we will show the diffusion path and diffusion activation energy of copper atoms in the structure of anti-fluorite Be_2C. The $2\times2\times2$ super-cell of anti-fluorite Be_2C and $3\times3\times3$ k-point scheme were used.

3. Results and discussion

3.1. Diffusion barrier of copper atoms in beryllium crystal

The lattice constants a and c of beryllium crystal were calculated to be $a = 2.24$ Å and $c = 3.53$ Å compared with the experimental values $a = 2.29$ Å, $c = 3.58$ Å.[34] As shown in Table 1, we obtained the formation energy of the interstitial and substitutional copper atoms in the crystal of beryllium, as well as the Frenkel disorder and Schottky disorder. The Schottky vacancy formation energy is 1.09 eV reported by Middleburgh[31] in the crystal of beryllium, and the intrinsic concentration of vacancies is 3.21×10^{-6} at 1000 K. The formation energy of Frank disorder is larger than 5 eV, which indicates that the intrinsic concentration of Frank vacancies is lower than the Schottky vacancies. Huang *et al.*[35] found that copper diffused into the crystal of beryllium with a concentration of about 0.06 at.% between the interfaces 0 at.% and 1.0 at.% layers in the experiment, which is much larger than the intrinsic vacancy concentration in the crystal. As shown in Table 1, although the formation energy of copper atom at the substitution site is the lowest, it is difficult for the crystal of beryllium to form self-interstitial atoms (Frank disorder is larger than 5 eV), so there is no need to consider the kick-out mechanism. Therefore, we consider the two diffusion mechanisms of interstitial and vacancy when calculating

the diffusion activation energy of the copper atom. We consider three diffusion networks in the interstitial mechanism, which are Tr–Oc–Tr (0.87 eV), Tr–Hx–Tr (1.03 eV), and Tr–NBt–Tr (0.79 eV), as shown in Figs. 2(a), 2(b), and 2(c). Our results indicate that the Cu atoms diffusion perpendicular to the hexagonal axis (diffusion barrier 0.79) is easier than that parallel to the hexagonal axis (diffusion barrier 0.87) in the crystal of beryllium, which is consistent with the results of Butrymowicz.[36] We also calculated the diffusion activation energy of copper atoms through three diffusion paths in the vacancy mechanism, there are pathway-I (0.89 eV), pathway-II (0.93 eV), and pathway-III (3.85 eV), as shown in Figs. 2(d), 2(e), and 2(f). It is indicated that the copper atom can easily jump to the nearest vacancy in the vacancy mechanism, but it is difficult to jump to the second nearest neighbor vacancy. The activation energy of copper atoms diffused by the interstitial mechanism is only 0.10 eV, less than the vacancy mechanism. Therefore, the initial and final states of the copper atoms were set in the beryllium crystal interstitial position (Tr) when calculating diffusion activation energy of the copper atoms later in this paper.

Table 1. The formation energy of single point defect in the crystal of beryllium calculated using a $4\times4\times3$ supercell.

Defect	Defect type	Formation energies/eV
Vacancy	–	1.064
Interstitial	basal trigonal site (Tr)	1.111
	basal hexahedral site (Hx)	2.070
	non-basal octahedral site (Oc)	1.977
	non-basal tetrahedral site (Te)	1.589
	non-basal trigonal site (NBt)	1.437
Substitution	Be-and-subCu	−3.885
Frenkel	bound	5.208

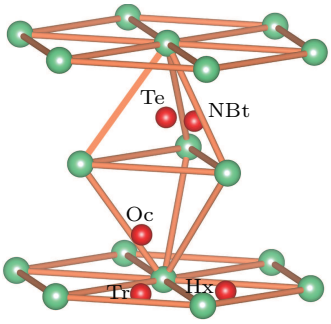


Fig. 1. The five interstitial sites of copper atom are in the crystal of beryllium: trigonal interstitial site (Tr), and hexahedral site (Hx) in the base plane; octahedral site (Oc), tetrahedral site (Te), and non-basal trigonal interstitial site (NBt) in the non-base plane.

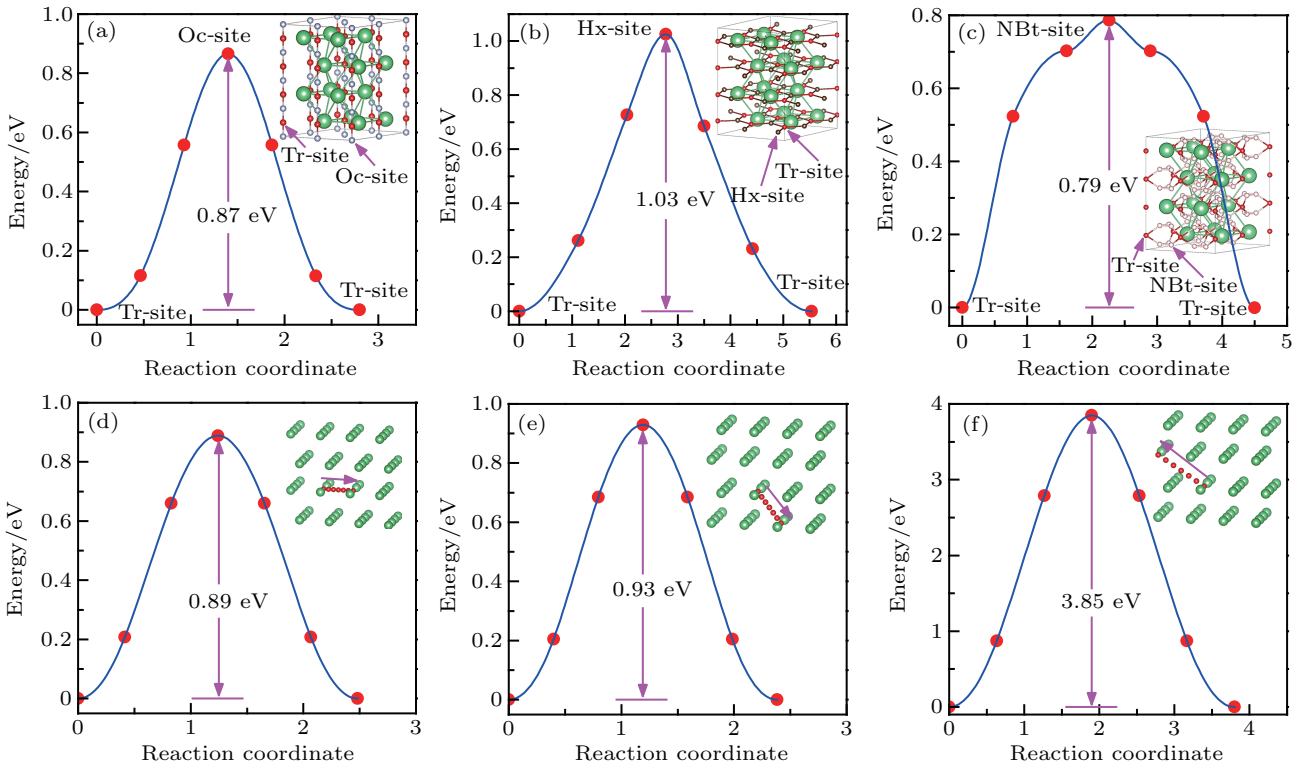


Fig. 2. Diffusion activation energy and configuration diagram of three diffusion networks of interstitial copper atoms in the crystal of beryllium: (a) Tr–Oc–Tr, (b) Tr–Hx–Tr, (c) Tr–NBt–Tr. Diffusion of copper atoms in the crystals of beryllium by vacancy mechanism: (d) pathway-I, (e) pathway-II, (f) pathway-III.

3.2. Adsorption of copper on the surface of Be_2C-I and diffusion barrier

The two-dimensional beryllium carbide (Be_2C-I) was predicted by Li *et al.*[21] and its melting point was estimated to be between 1500 K and 2000 K by using first-principles molecular dynamics simulations. The pyrolysis condition of the Be–Cu capsule is 698 K,[9] so the thermal stability of this two-dimensional material is sufficient to withstand the pyrolysis temperature. The lattice constant after relaxation is $a = 2.98$ Å, the C–Be and Be-Be bond lengths are 1.78 Å

and 1.96 Å, and the Be–C–Be bond angle is 66.6°, which is in agreement with the result of Li *et al.*[21] Their results are the following: $a = 2.99$ Å, C–Be and Be–Be bond length are 1.73 Å and 1.98 Å, and the Be–C–Be bond angle is 66.5°. The adsorption energy of copper atoms was calculated on the surface of Be_2C-I in order to configure the initial structure of CINEB. The adsorption sites are shown in Fig. 3, the Be-1, Be-2, and C sites are at the top of the corresponding Be and C atoms, and the hollow-1, hollow-2, and hollow-3 sites are located at the hollow site formed by the corresponding atoms, respectively. As shown in Table 2, the adsorption energy of copper atoms on the surface of Be_2C-I are negative, which indicates that the adsorption of copper atoms is stable. The site of C is the most favorable for the copper atom adsorbing on the surface of Be_2C-I, and the largest difference of the adsorption energies among these six sites is about 0.649 eV. So, we set the initial state at the site of C when calculating the diffusion barrier of copper atom through the Be_2C-I monolayer. We also calculated the diffusion barrier of copper atom when the Be_2C-I monolayer is inside the crystal of beryllium. As shown in Fig. 4, it is necessary to overcome the energy barrier not less than 2.85 eV as the copper atoms diffuse through the Be_2C-I monolayer. The energy profile near Be_2C-I monolayer is very low, as shown in Fig. 4(b), and the maximum energy drop is 3.92 eV, which means that copper atoms near the Be_2C layer will be difficult to jump into the crystal of beryllium. This may be an effective barrier to the diffusion of copper atom in the capsule, because the diffusion barrier of copper atoms in the crystal of beryllium is only 0.79 eV.

Table 2. The adsorption energy (E_{ad}) and the adsorption height (h_{cu}) of Cu at different positions of Be_2C-I.

Site	E_{ad}/eV	h_{cu}/Å
Be1	−1.265	2.235
Be2	−1.677	1.458
C	−1.914	1.595
Hollow-1	−1.900	1.642
Hollow-2	−1.865	1.645
Hollow-3	−1.677	1.644

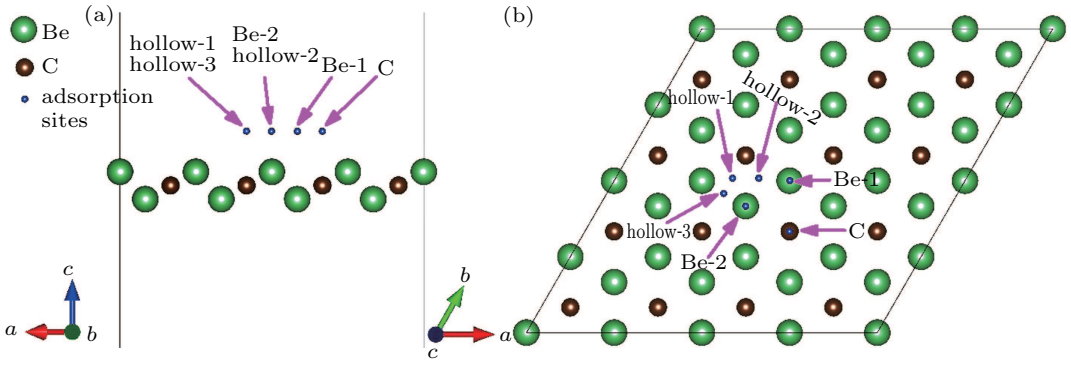


Fig. 3. The Be_2C-I monolayer structure and the adsorption sites of copper atom on its surface: (a) side view; (b) top view.

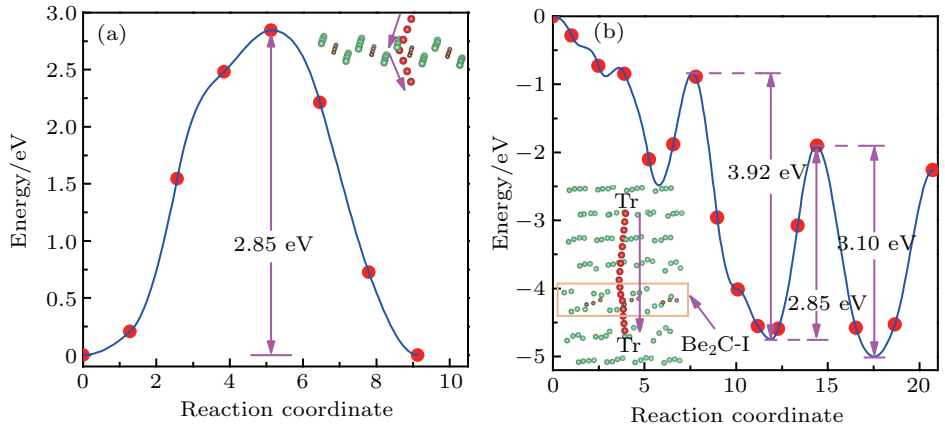


Fig. 4. The diffusion barrier of copper atoms as they pass through the Be_2C-I monolayer and the monolayers are placed in the crystal of beryllium: (a) Be_2C-I monolayer, (b) the Be_2C-I monolayer in the crystal of beryllium.

3.3. Adsorption of copper atoms on the surface of Be_2C-III and diffusion barrier

Mosayeb *et al.*[22] predicted two-dimensional Be_2C-III structure by using the method of first-principles. The melting point of the monolayer layer is close to 1500 K. This temperature is also fully tolerable in the pyrolysis conditions of the beryllium ablator capsules. The final results of our lattice relaxation are: $a = 4.93$ Å, $b = 2.97$ Å, the plane spacing of two layers of carbon atoms and beryllium atoms are: $d_{cc} = 0.82$ Å, $d_{BeBe} = 1.17$ Å. This is consistent with

the results of Mosayeb *et al.*:[22] $a = 5.00$ Å, $b = 2.99$ Å, $d_{cc} = 0.74$ Å, $d_{BeBe} = 1.12$ Å. Similarly, the adsorption energy of copper atoms was calculated as in Subsection 3.2. The adsorption sites are shown in Fig. 5, the Be-1, Be-2, C-1, and C-2 sites are at the top of the corresponding Be and C atoms, and the bridge-1 and bridge-2 sites are at the bridge site formed by two Be atoms in a plane, respectively. As shown in Table 3, the adsorption energy of copper atoms on the surface of Be_2C-III is all negative, so copper atoms are easily stabilized on the surface. The largest difference of adsorption energies among these six sites is about 0.599 eV. The site of bridge-2 is the most favorable for the copper atom adsorbing on the surface of Be_2C-III monolayer. Therefore, we configure the initial state at the site of bridge-2 when calculating the diffusion barrier of copper atoms through the Be_2C-III monolayer. We set the initial position of copper atom at the trigonal site (Tr) when the Be_2C-III monolayer is inside the crystal of beryllium, because the formation energy corresponding to this site is minimal. As shown in Fig. 6, the results indicate that the copper atoms need to overcome the energy barrier of 5.14 eV and 6.09 eV, respectively, when passing through the Be_2C-III monolayer and inside the crystal of beryllium. This energy barrier (6.09 eV) is very high compared to that in the crystal of beryllium (0.79 eV). Therefore, Be_2C-III can also effectively prevent the diffusion of copper atoms, which is a reasonable copper diffusion barrier material in the capsule.

Table 3. The adsorption energy (E_{ad}) and the adsorption height (h_{cu}) of copper atoms at different positions of Be_2C-III.

Site	E_{ad}/eV	h_{cu}/Å
C-1	−1.847	1.791
C-2	−1.824	1.888
Be-1	−1.357	2.147
Be-2	−1.938	1.348
Bridge-1	−1.457	1.983
Bridge-2	−1.956	1.115

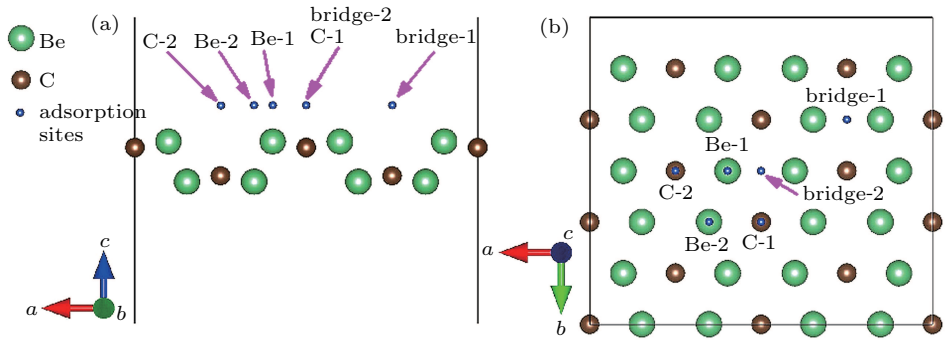


Fig. 5. The Be_2C-III monolayer structure and the adsorption sites of copper atoms on its surface: (a) side view; (b) top view.

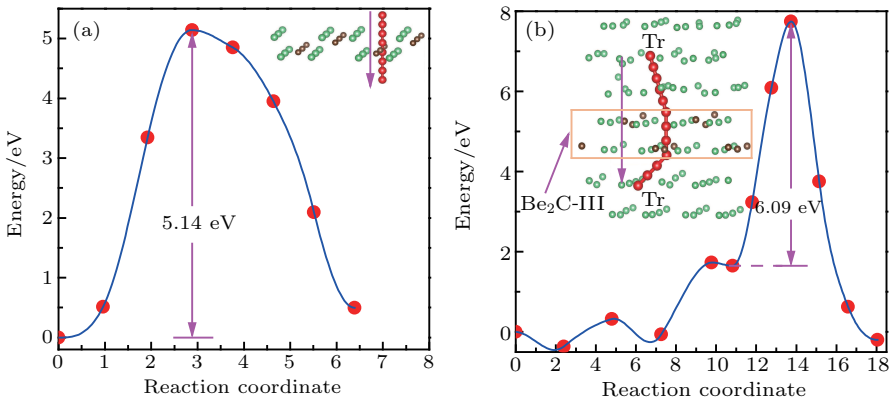


Fig. 6. The diffusion barrier of copper atoms as they pass through the Be_2C-III monolayer and the monolayer is placed in the crystal of beryllium: (a) Be_2C-III monolayer, (b) the Be_2C-III monolayer in the crystal of beryllium.

3.4. Diffusion barrier of copper atom in anti-fluorite Be_2C

The structure of anti-fluorite Be_2C has been reported by Stackelberg and Quatram.[37] When the k-point reaches $6\times6\times6$, the energy fluctuation reaches the specified accuracy (less than 5 meV/atoms). The super-cells model of $2\times2\times2$ was utilized, so the Brillouin region was segmented using the k-point density of $3\times3\times3$. After relaxation of this anti-fluorite structure, the lattice constant is 4.29 Å, which is similar to the experimental value of 4.34 Å.[20] It is also in good agreement with other theoretical results, such as 4.29 Å given by Lee *et al.*,[38] and 4.335 Å given by Joshi *et al.*.[17] All the calculated lattice constants are slightly less than the experimental values. As shown in Fig. 7, we configure the initial structure of copper atoms as follows: the first nearest neighbor of the initial state is a cubic hexahedron surrounded by eight beryllium atoms, and the second nearest neighbor is a regular octahedron surrounded by six carbon atoms. After relaxation, the distance between the copper atoms of the initial

and final structures is 3.1 Å, and five transition structures are inserted therein using the method of linear interpolation. The results show that the diffusion of copper atoms in the anti-fluorite Be_2C needs to overcome the energy barrier of 2.95 eV, as shown in Fig. 7. This barrier is much higher than the copper atoms in the single crystal beryllium (0.79 eV). The thickness of each layer is on the order of microns when designing the capsule. Therefore, placing a certain thickness of Be_2C at the capsule interface may effectively block the diffusion of copper atoms into the interior of the crystal of beryllium.

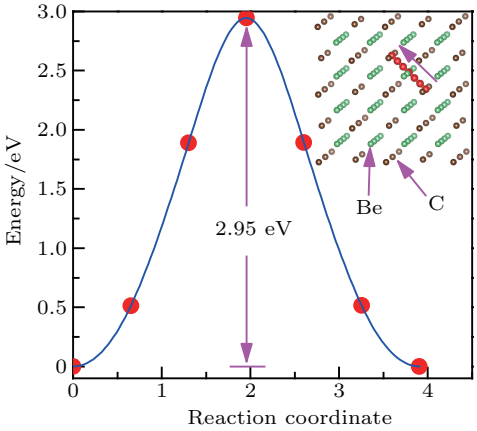


Fig. 7. The diffusion barrier of copper atom in perfect anti-fluorite Be_2C.

4. Conclusions

In summary, based on the density functional theory, we calculated the diffusion activation energy of copper atoms in the crystal of beryllium and beryllium carbide, and the adsorption energy of copper atom on the surface of two-dimensional beryllium carbide (Be_2C-I and Be_2C-III). The results show that the adsorptions of copper atoms on the surface of Be_2C-I and Be_2C-III are stable, and optimal adsorption sites are on the top of the carbon atoms (C) and the bridge site formed by the first layer of beryllium atoms (bridge-2), respectively. We also calculated the point defects formation energy in the crystal of beryllium. The formation energy is the lowest when the copper atom is in the substitutional sites, and the second one is in the site of the trigonal interstitial site (Tr). The diffusion activation energy of copper atoms in the crystal of beryllium was investigated. The diffusion activation energy of copper atoms is lower in interstitial mechanism than that of vacancy mechanism. Copper atoms need to overcome the barriers of 2.85 eV and 5.14 eV when passing through the Be_2C-I and Be_2C-III monolayers, while they are 2.85 eV and 6.09 eV when two-dimensional Be_2C was embedded in the crystal of beryllium, respectively. This is very large relative to the diffusion activation energy of copper atoms in the crystal of beryllium. Therefore, beryllium carbide monolayer can effectively block the diffusion of copper atom in capsule. The diffusion activation energy of copper atoms in the anti-fluorite Be_2C is 2.95 eV, which is also significantly larger than that in the crystal of beryllium. Our research shows that the three structures of beryllium carbide can effectively block copper diffusion. This is very useful for the preparation of higher performance capsule.

References

[1] Mitteau R, Stangeby P, Lowry C, Firdaouss M, Labidi H, Loarte A, Merola M, Pitts R and Raffray R 2011 *J. Nucl. Mater.* **415** S969
[2] Spilker B, Linke J, Loewenhoff T, Pintsuk G and Wirtz M 2017 *Nucl. Mater. Energy* **12** 1184
[3] Kline J, A Yi S, Simakov A, *et al.* 2016 *Phys. Plasmas* **23** 056310
[4] Wilson D C, Bradley P A, Hoffman N M, Swenson F J, Smitherman D P, Chrien R E, Margevicius R W, Thoma D J, Foreman L R, Hoffer J K, Goldman S R, Caldwell S E, Dittrich T R, Haan S W, Marinak M M, Pollaine S M and Sanchez J J 1998 *Phys. Plasmas* **5** 1953
[5] Moses E I, Boyd R N, Remington B A, Keane C J and Al-Ayat R 2009 *Phys. Plasmas* **16** 041006
[6] Zylstra A B, Yi S A, MacLaren S, *et al.* 2018 *Phys. Plasmas* **25** 102704
[7] MacKinnon A J, Meezan N B, Ross J S, *et al.* 2014 *Phys. Plasmas* **21** 056318
[8] Simakov A N, Wilson D C, Yi S A, Kline J L, Clark D S, Milovich J L, Salmonson J D and Batha S H 2014 *Phys. Plasmas* **21** 022701
[9] Youngblood K P, Huang H, Xu H W, Hayes J, Moreno K A, Wu J J, Nikroo A, Alford C A, Hamza A V, Kucheyev S O, Wang Y M and Wu K J 2013 *Fusion Sci. Technol.* **63** 208
[10] Xu H, Youngblood K P, Huang H, Wu J J, Moreno K A, Nikroo A, Shin S J, Wang Y M and Hamza A V 2013 *Fusion Sci. Technol.* **63** 202
[11] Rovner L H and Hopkins G R 1976 *Nucl. Technol.* **29** 274
[12] Liu X, Cheng X L and Lu Y P 2017 *Phys. Lett. A* **381** 3211
[13] Anghel A, Porosnicu C, Lungu C P, Sugiyama K, Krieger C and Roth J 2011 *J. Nucl. Mater.* **416** 9
[14] Kost F, Linsmeier C, Oberkofler M, Reinelt M, Balden M, Herrmann A and Lindig S 2009 *J. Nucl. Mater.* **390–391** 975
[15] Mateus R, Carvalho P A, Franco N, Alves L C, Fonseca M, Porosnicu C, Lungu C P and Alves E 2013 *J. Nucl. Mater.* **442** S320
[16] Luo B C, Zhang J Q, He Y D, Chen L, Luo J S, Li K and Wu W D 2017 *High Power Laser Sci.* **5** e10
[17] Joshi K B, Trivedi D K, Paliwal U and Galav K L 2016 *Mater. Res. Express* **3** 055601
[18] Tzeng C T, Tsuei K D and Lo W S 1998 *Phys. Rev. B* **58** 6837
[19] Shih W S, Stephens R B and James W J 2000 *Fusion Sci. Technol.* **37** 24
[20] Wyckoff R W G 1963 *Crystal Structures*, Vol. 1, 2nd edn. (New York: Interscience)
[21] Li Y F, Liao Y L and Chen Z F 2014 *Angew. Chem. Int. Edit.* **53** 7248
[22] Naseri M, Jalilian J, Parandin F and Salehi K 2018 *Phys. Lett. A* **382** 2144
[23] Henkelman G and Jónsson H 2000 *J. Chem. Phys.* **113** 9978
[24] Henkelman G, Uberuaga B P and Jónsson H 2000 *J. Chem. Phys.* **113** 9901
[25] Kresse G and Joubert D 1999 *Phys. Rev. B* **59** 1758
[26] Kresse G and Furthmüller J 1996 *Phys. Rev. B* **54** 11169
[27] Perdew J P, Burke K and Ernzerhof M 1996 *Phys. Rev. Lett.* **77** 3865
[28] Monkhorst H J and Pack J D 1976 *Phys. Rev. B* **13** 5188
[29] Bučko T, Hafner J, Lebègue S and Ángyán J G 2010 *J. Phys. Chem. A* **114** 11814
[30] Krimmel H and Fähnle M 1996 *J. Nucl. Mater.* **231** 159
[31] Middleburgh S C and Grimes R W 2011 *Acta Mater.* **59** 7095
[32] Zhang X, Li X, Wu P, Chen S, Zhang S, Chen N and Huai X 2018 *Curr. Appl. Phys.* **18** 1108
[33] Liu H, Dong H, Ji Y, Wang L, Hou T and Li Y 2019 *Appl. Surf. Sci.* **466** 737
[34] Ashcroft N W and Mermin N D 1976 *Solid State Physics* (New York: Cornell University) p. 77
[35] Huang H, Xu H W, Youngblood K P, Wall D R, Stephens R B, Moreno K A, Nikroo A, Wu K J, Wang M and Hamza A V 2013 *Fusion. Sci. Technol.* **63** 190
[36] Butrymowicz D B, Manning J R and Read M E 1975 *J. Phys. Chem. Ref. Data* **4** 177
[37] Stackelberg M V and Quatram F 1934 *Z. Physik. Chem.* **27** 50
[38] Lee C H, Lambrecht W R L and Segall B 1995 *Phys. Rev. B* **51** 10392